THESIS

INCORPORATING VEHICLE TRAILS IN SOIL MOISTURE DOWNSCALING FOR MOBILITY ASSESSMENTS IN COARSE GRAINED SOILS

Submitted by

Holly E. Proulx

Department of Civil and Environmental Engineering

In partial fulfillment of the requirements

For the Degree of Master of Science

Colorado State University

Fort Collins, Colorado

Spring 2024

Master's Committee:

Advisor: Jeffrey D. Niemann
Co-Advisor: Joseph Scalia

Stacy Lynn

ABSTRACT

INCORPORATING VEHICLE TRAILS IN SOIL MOISTURE DOWNSCALING FOR MOBILITY ASSESSMENTS IN COARSE GRAINED SOILS

Fine resolution (10-30 m) soil moisture maps are critical for determining vehicle mobility in agricultural, forestry, recreational, and military applications. Microwave satellites provide soil moisture products, but the spatial resolutions of these products are too coarse for such applications. Soil moisture downscaling methods, such as the Equilibrium Moisture from Topography Plus Vegetation and Soil (EMT+VS) model, can downscale soil moisture to fine resolutions. However, the EMT+VS model (like most other downscaling models) does not explicitly consider vehicle trails, which may have different soil moisture than undisturbed landscape locations. The objective of this study is to generalize the EMT+VS model to explicitly estimate the soil moisture of trails. The generalized model incorporates two hypothesized effects of vehicle traffic on trails (reduced vegetation cover and reduced porosity). To evaluate the generalized model, porosity and soil moisture observations were collected across a study region in the foothills of the Colorado Front Range. Data were collected at paired trail and landscape locations as well as unpaired landscape locations on six dates in Summer 2023. On average, the porosity of the trail locations was 86% of the paired landscape locations. Soil moisture on trails was on average 73% to 88% of the moisture of the paired landscape locations. Including the vegetation and porosity adjustments in the EMT+VS model reduced the tendency of the model to overestimate the moisture on trails and improved the root mean squared errors.

ACKNOWLEDGEMENTS

This research was sponsored by the Army Research Laboratory and was accomplished under Cooperative Agreement Number W911NF-21-2-0252. The views and conclusions contained in this document are those of the authors and should not be interpreted as representing the official policies, either expressed or implied, of the Army Research Office or the U.S. Government. Additional funding was provided by USDA National Institute for Food and Agriculture, Hatch grant 1000065-COL00797, and the National Science Foundation (2312319). I thank my attentive advisors, Dr. Jeffrey Niemann and Dr. Joseph Scalia, for their endless guidance and support throughout this project. I also thank Tim Green of the USDA-ARS, for his input and knowledge. I thank Dr. Stacy Lynn for her additional perspective and for serving on my master's committee. I acknowledge Joel Vaad and CSU Strata for coordinating access to Maxwell Ranch. I thank Samantha Fischer and Boran Kim for their assistance with field data collection and the EMT+VS MATLAB code. I thank Joseph Bindner, Cecilia Brockett, Holly Ho, Samuel Jacob, Kendall Monley, Kaylee Romero, and Alec Shields for their assistance with field data collection and countless hours in the laboratory analyzing soil samples.

TABLE OF CONTENTS

1 INTRODUCTION

Soil moisture, or volumetric water content, is an important variable for many applications including climate and weather forecasting, water management, wildfire prediction, and vehicle mobility assessments (Dobriyal, 2012). Vehicle mobility assessments are needed for agricultural, forestry, recreational, and military activities including both frontline fighting and disaster relief (Hestera, 2018). To be useful for mobility applications, soil moisture estimates must span large geographic regions (e.g., ~10-km extents), have fine spatial resolution (e.g., ~10 m grid cells), and consider both undisturbed landscape locations and vehicle trails. A vehicle trail refers to any trail created by and used for vehicles from native soil without engineered improvements. Trails are important in mobility applications because they are often preferred travel routes.

The hydrology of trails can differ from the undisturbed landscape due to the vehicular traffic, which causes compaction. Botta et al. (2009) showed that trails experience the most compaction within the first four to five vehicle passes in clayey soils of former agricultural fields. Trails with at least five passes were considered well-developed because their density tended to stabilize irrespective of further vehicle traffic. Compaction can cause trails to have increased bulk density (Najafi et al., 2010), decreased porosity (Hansson et al., 2019), and decreased infiltration capacity (Johnson et al., 1980). Each of these phenomena were shown in studies conducted on forest soils. Additionally, trails can serve as preferential paths for surface runoff and sediment transport, as modeled at agricultural fields by Heathwaite et al. (2005). The hydrology of trails can also be influenced by rutting from vehicle traffic (Sadeghi et al., 2022). Hansson et al. (2019) found that decreased vegetation on trails can lead to higher soil moisture

when compared to nearby undisturbed areas. This was shown on glacial till soils with high stone and boulder content (50% of the soil consisted of rocks with diameters >20 mm).

Soil moisture can be obtained for mobility applications by downscaling estimates from microwave satellites. These satellites provide frequent (e.g., 3-day intervals) soil moisture estimates over large spatial extents (Peng et al., 2021). However, the data has coarse resolutions. The European Space Agency's Soil Moisture and Ocean Salinity (SMOS) satellite has 40 km resolution, NASA's Advanced Microwave Scanning Radiometer Eos (AMSR-E) has 15 km resolution, and NASA's Soil Moisture Active Passive (SMAP) has 9 km resolution (some products from these satellites have other resolutions). To reach fine spatial resolutions, downscaling is needed. Various soil moisture downscaling methodologies have been proposed, which can be categorized by the fine resolution data they emphasize when inferring the fine resolution variations of soil moisture or the downscaling methodology employed. Comprehensive reviews of such downscaling methods are provided by Sabaghy et al. (2018) and Peng et al. (2021).

Focusing on the fine-resolution datasets that are used, downscaling methods can be classified as radar, optical/thermal, or topographical methods. Radar-based downscaling uses fine-resolution active microwave data to supplement the coarse information from passive microwave radiometers (Bindlish et al, 2008, Wu et al, 2014). Optical/thermal methods use the visible and near-infrared parts of the spectrum to infer vegetation properties and thermal data to derive the land-surface temperature. For example, the triangle/trapezoid method uses optical/thermal data to define linear relationships between land surface temperature and soil moisture for use in downscaling (Merlin et al., 2006, Fang et al., 2013). Topographic methods infer spatial variations in soil moisture from topographic attributes that have been shown to

impact soil moisture (such as slope and drainage area) (Perry and Niemann, 2007; Ranney et al., 2015; Eylander et al., 2023).

From a methodological perspective, downscaling methods can be classified as either statistical, empirical, or mechanistic. Statistical methods focus on reproducing the statistical properties of fine-resolution soil moisture patterns (such as the range of values and the spatial correlation structure) rather than accurately estimating the soil moisture value at each location. Statistical methods include multifractal (Mascaro et al., 2010) and geostatistical (Deshon et al., 2020) approaches. Empirical methods infer the relationships between potential explanatory variables and soil moisture using fine-resolution soil moisture observations. These methods include empirical-orthogonal-function downscaling (Perry and Niemann, 2007), regression models (Loew and Mauser, 2008), random forest machine learning (Schönauer et al., 2023), support vector machines (Ahmad et al., 2010; Jin et al., 2020), and neural networks (Alemohammad et al., 2018; Xu et al., 2022). Mechanistic downscaling approaches emphasize the physical processes that govern soil moisture dynamics. For example, GeoWATCH is a data assimilation method that uses static (DEM, soil texture, land use) and dynamic (meteorological) datasets to downscale soil moisture (Eylander et al., 2023).

The Equilibrium Moisture from Topography Plus Vegetation and Soil (EMT+VS) model is among the most studied downscaling methods. The EMT+VS model uses a mechanistic approach to infer soil moisture variations and fine-resolution topographic, vegetation, and soil attributes. The model was originally developed for small catchments and has been shown to reproduce temporally varying spatial structures of soil moisture (Coleman and Niemann, 2013) and observed dependencies on vegetation and soil characteristics (Ranney et al., 2015). Because the EMT+VS model is mechanistic, it can outperform empirical models when calibration data

are limited (Werbylo and Niemann, 2014). Cowley et al. (2017) and Hoehn et al. (2017) extended the model to apply to large regions by modeling spatial variations in precipitation and potential evapotranspiration and allowing multiple coarse resolution grid cells. Grieco et al. (2018) proposed and tested methods for parameter estimation when field measurements of soil moisture are unavailable for calibration, and Pauly et al. (2020) evaluated key model assumptions related to runoff production and residual water content. Deshon et al. (2020) added a stochastic component to the EMT+VS model that simulates random fluctuations in soil moisture, and Fischer (2024) examined the model performance when using different input datasets. Pauly (2019), Bindner (2020), and Bullock (2023) used soil moisture from the EMT+VS model in a soil strength model designed for mobility assessments (the STRength of Surface Soils, STRESS, model). However, the current EMT+VS model focuses on estimating soil moisture at undisturbed landscape regions and ignores the potential impacts of trails on soil moisture.

Schönauer et al. (2023) used a random forest algorithm to downscale soil moisture on and near forest trails that are sensitive to machine traffic. They collected soil moisture observations with a portable moisture meter (6 cm depth) and a permanent soil sensor network (10 cm depth). A variety of topographic indices, temporal data, and soil data were considered as potential explanatory variables for the downscaling method. However, depth-to-water (a topographic index) and temporal information (year, month, season) had the highest correlations with the soil moisture observations and were selected as inputs. The coarse-resolution soil moisture input was a 9x9 km product from ERA5-Land, which combines ground-based and satellite-derived data using reanalysis. The downscaling model predicted observed soil moisture with a Kendall's correlation coefficient of 0.64. The modeled soil moisture data also predicted the measured rut

depths with a Kendall's correlation coefficient of 0.63. The study did not provide a direct comparison of soil moisture modeling capabilities at trails and landscape points. Also, the modeling approach is empirical, so it may not apply to other regions with different physical characteristics.

The objective of this study is to predict soil moisture on trails by generalizing the EMT+VS model framework. The EMT+VS model is selected due to its mechanistic basis and extensive prior evaluation. Based on the reviewed literature, the primary impacts of the vehicle traffic are hypothesized to be reductions in vegetation cover and porosity. However, the net effect of these impacts on the soil moisture of trails is unclear (Figure 1). The EMT+VS model is generalized to include these two hypothesized effects and applied to Maxwell Ranch (an active cattle ranch in the foothills of the Front Range in northern Colorado). To evaluate the model performance, porosity and in-situ soil moisture observations were collected at paired trail and landscape locations. Soil moisture observations were also collected at unpaired landscape locations across the study region.

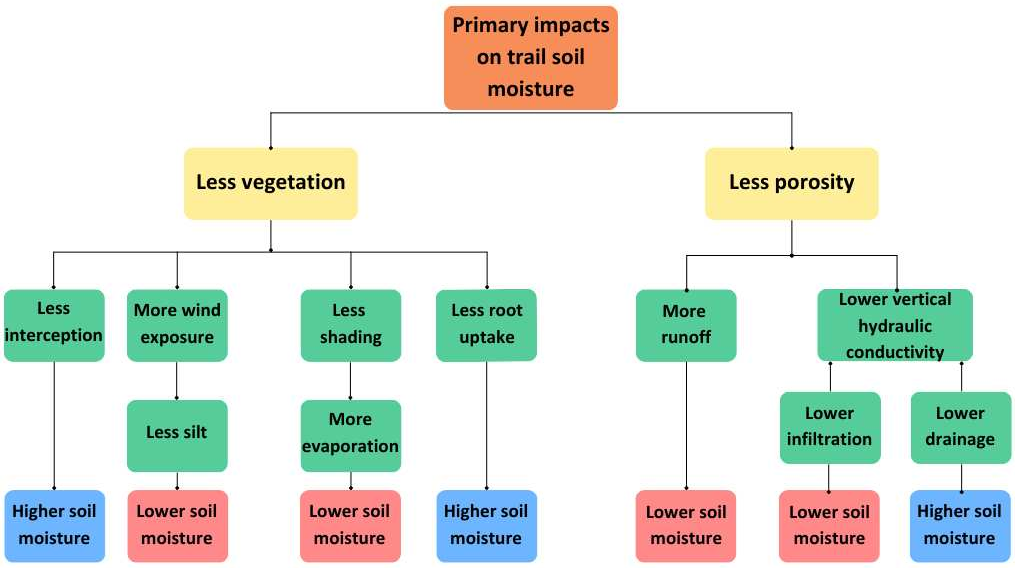

Figure 1. Conceptual diagram illustrating the hypotheses of how a well-developed trail can impact soil moisture.

2 MATERIALS AND METHODS

2.1 Pre-Existing EMT+VS Model

The EMT+VS model is based on a water balance of the surface soil layer and considers infiltration, deep drainage, lateral flow, and evapotranspiration. Infiltration F (mm/day) is based on the average precipitation $\bar{P}$ within the coarse resolution grid cells and accounts for interception by vegetation using:

$$F = \bar{P}(1 - \lambda V) \tag{1}$$

where V is the fractional vegetation cover and λ is the canopy interception efficiency. $\bar{P}$ eventually cancels out of the model equations, so it does not need to be specified. Equation (1) neglects runoff. Pauly et al. (2020) considered a generalized infiltration equation that accounts for runoff and found only minor improvements in the EMT+VS soil moisture estimates for undisturbed landscape locations. We also tested that equation for trails and found only minor improvements in the soil moisture estimates. Thus, runoff was left out for simplicity.

Deep drainage G (mm/day) is characterized using Darcy's Law and assumes vertical flow is gravity driven. The unsaturated hydraulic conductivity is determined using the Campbell (1974) equation, and the porosity depends on the vegetation cover to account for the effect of organic matter (Fischer, 2024). The resulting equation is:

$$G = K_{s,v}\left(\frac{\theta}{\phi + \chi V}\right)^{\gamma_v} \tag{2}$$

where $K_{s,v}$ is the vertical saturated hydraulic conductivity (mm/day), θ is the fine-resolution soil moisture, γ_v is the vertical pore disconnected index, ϕ is the bare soil porosity, and χ adjusts the bare soil porosity to account for organic matter.

Lateral flow L (m^2mm/day) is also described using Darcy's Law and the Campbell (1974) equation. The lateral flow equation accounts for anisotropy of the soil and assumes that the lateral hydraulic gradient is related to the topographic slope. The thickness of the soil layer is assumed to depend on the topographic curvature. The resulting equation is:

$$L = \delta_0 \left(\frac{\kappa_{min}-\kappa}{\kappa_{min}}\right) c\iota K_{s,v} \left(\frac{\theta}{\phi+\chi V}\right)^{\gamma_h} S^{\epsilon} \quad (3)$$

where δ_0 is the thickness of the hydrologically active layer (m) where topographic curvature is zero, κ_{min} is the minimum topographic curvature that has the soil layer, and κ is the topographic curvature (positive for convergent terrain and negative for divergent terrain). The variable c (m) is the length of the digital elevation model (DEM) grid cells (and the spatial resolution of the fine-resolution soil moisture estimates). The parameter ι is the anisotropy of the saturated hydraulic conductivity, which is used to transform $K_{s,v}$ to the horizontal saturated hydraulic conductivity. The parameter γ_h is the horizontal pore disconnectedness index, S is the topographic slope, and ϵ is a parameter relating the horizontal hydraulic gradient to the topographic slope.

Evapotranspiration E (mm/day) is calculated using:

$$E = \overline{E_p}[1 + \omega(\bar{Z} - Z)][\eta V + (1 - V)^{\mu}] \left[\frac{I_p}{1+\alpha}\left(\frac{\theta}{\phi+\chi V}\right)^{\beta_r} + \frac{\alpha}{1+\alpha}\left(\frac{\theta}{\phi+\chi V}\right)^{\beta_a}\right] \quad (4)$$

where $\overline{E_p}$ is the spatial average potential evapotranspiration within a coarse resolution grid cell (mm/day). The first bracketed term adds fine resolution variability to the potential evapotranspiration using elevation variations. The parameter ω controls elevation dependence, Z is the local elevation (m), and $\bar{Z}$ is the spatial average elevation within the coarse resolution grid cell. The second bracketed term describes the effect of the fractional vegetation cover on the transpiration and evaporation. The parameter η is the portion of the transpiration that is from the

modeled soil layer, and μ describes the effect of vegetation shading on soil evaporation. The third bracketed term includes the radiative and aerodynamic contributions to the total evapotranspiration. The variable I_p is the potential solar radiation index, which is calculated using the slope and aspect from the DEM, α is the Priestly-Taylor coefficient minus one, β_r describes the effect of moisture limitations on radiative evapotranspiration, and β_a describes the effect of moisture limitations on aerodynamic evapotranspiration.

The fine resolution soil moisture is calculated by a weighted average of four analytical soil moisture estimates:

$$\theta = \frac{w_G\theta_G + w_L\theta_L + w_R\theta_R + w_A\theta_A}{w_G + w_L + w_R + w_A} \quad (5)$$

where θ_G, θ_L, θ_R, and θ_A are the analytical soil moisture estimates when deep drainage, lateral flow, radiative evapotranspiration, and aerodynamic evapotranspiration dominate the water balance, respectively. The weights w_G, w_L, w_R, and w_A are determined from the magnitudes of those four processes in the water balance (Ranney et al., 2015).

In the end, the EMT+VS model requires fine-resolution vegetation and topographic data (and can optionally use fine resolution soil data) along with a coarse resolution grid soil moisture (or single average soil moisture value) to determine all the terms in the weighted average. The EMT+VS model also requires specification of the 16 parameters. Ranney et al. (2015) and Cowley et al. (2017) provide more details about the derivation as well as the analytical solutions that are used in the weighted average.

2.2 Incorporation of Trail Hypotheses in the EMT+VS Model

The locations of trails are assumed to be known before applying the EMT+VS model. To incorporate trails in the model, a binary raster is used to indicate whether a trail is present in each fine-resolution grid cell. This raster is denoted T and has a value of 1 in cells where trails occur

and 0 for all other (undisturbed landscape) cells. As discussed earlier, vehicle traffic is expected to reduce the vegetation cover on trails. Because the fine-resolution grid cell (10 m) is typically larger than the trails (~2-5 m), the uncorrected vegetation cover of a trail cell reflects a combination of the trail and landscape conditions. To explicitly consider the conditions of the trail, the fractional vegetation cover of each trail cell (where $T = 1$) is set to:

$$V_T = \zeta_T V \tag{6}$$

where V_T is the trail-adjusted fractional vegetation cover and ζ_T describes the impact of the vehicle traffic on the vegetation cover (V is the original fractional vegetation cover of the cell). Similarly, vehicle traffic is also expected to compact the soil of the trail, which reduces the porosity. Thus, the (bare soil) porosity of each trail cell (where $T = 1$) is set to:

$$\phi_T = \rho_T \phi \tag{7}$$

where ϕ_T is the trail-adjusted porosity and ρ_T describes the effect of vehicle traffic on the porosity (ϕ is the original porosity, which describes undisturbed conditions). Both ζ_T and ρ_T are new trail-related parameters that need to be calibrated.

2.3 Study Area

Maxwell Ranch is a 4000-ha cattle ranch in the Laramie Foothills in northern Colorado (Figure 2). This region has been previously used for testing the EMT+VS model (Fischer, 2024) and an associated soil strength model (Bullock, 2023) at undisturbed locations. Maxwell Ranch has an average elevation of ~2,210 m and minimum and maximum elevations of 1,960 and 2,290 m, respectively. The soils across Maxwell Ranch are primarily thin gravelly sandy loams derived mostly from weathered granite (Soil Survey Staff, 2022; Bullock, 2023). Peats occur in some valley bottoms (Bullock, 2023; Fischer, 2024). The vegetation consists of short-grass

prairies with scattered shrubs and Ponderosa Pine trees. The site has ~46 km of trails that are double track, comprised of native soils, and traversed by ranch vehicles (pickup trucks) and occasional horse traffic. These trails are considered well-developed as they pre-date Google Earth imagery from 1985 and have therefore been trafficked for over 40 years (Google, 2022).

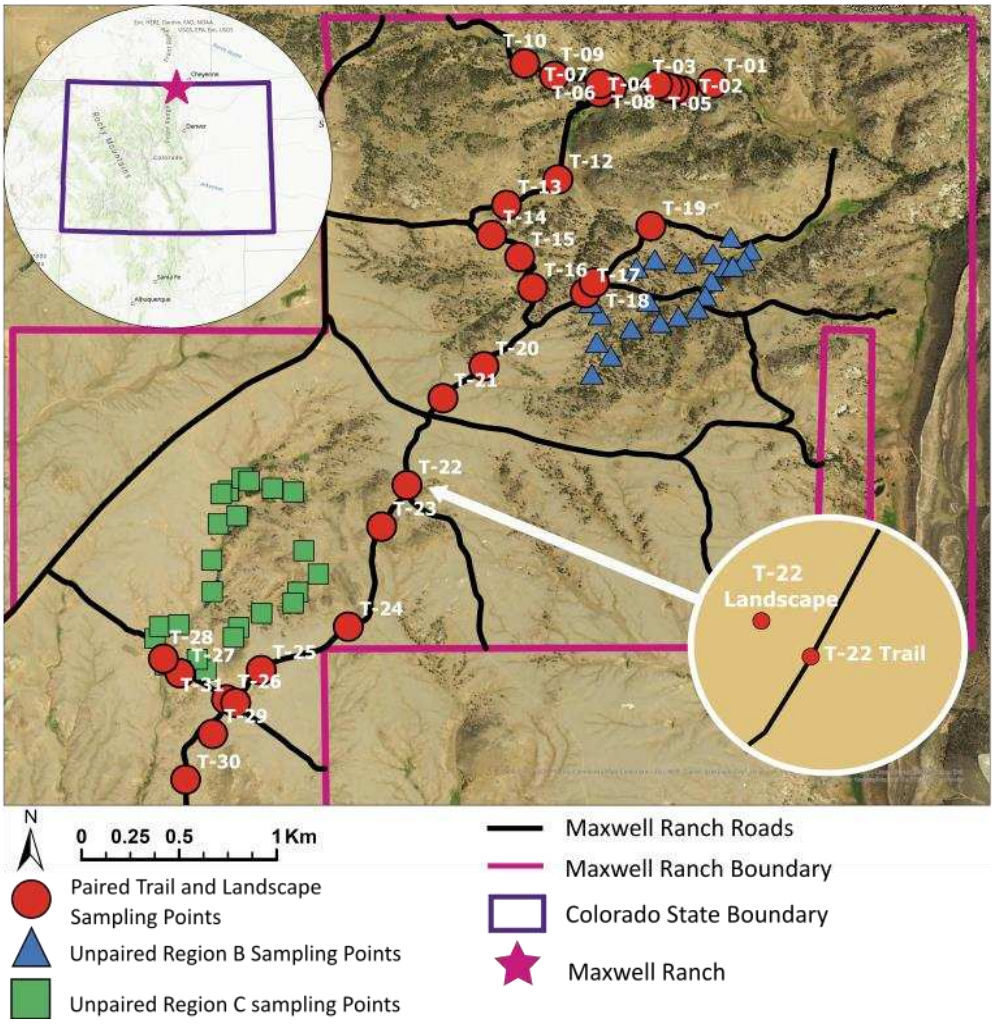

Figure 2. Map showing the sampling locations within the northern portion of Maxwell Ranch.

2.4 Sampling Location Selection

Figure 2 shows the sampling locations used in this study. Regions B and C were previously identified and used by Bullock (2023) and Fischer (2024). Within these two regions, they identified undisturbed sampling locations that span a diverse array of topographic,

vegetation, and soil conditions. Region B has 22 sampling locations, and Region C has 24 locations. These same locations are also used in the present study.

In addition, 30 paired trail and landscape sampling locations were identified for the present study. The trail locations were selected to observe trail conditions for diverse combinations of topographic, vegetation, and soil characteristics. Topographic attributes considered in the selection process included elevation, log of specific contributing area, slope, curvature, and cosine of aspect (topographic variables that appear in the EMT+VS model). The log transformation of specific contributing area is often used for hydrologic applications as it reduces the dominance of extreme values. Similarly, the cosine of aspect better represents the impact of solar radiation on slopes than aspect. Trail locations were initially selected using a Latin hypercube approach (Werbylo and Niemann, 2014) and then finalized based on field inspection. Trail sections with culverts or substantial rutting or erosion were avoided to reduce the number of trail factors influencing soil moisture.

Each trail location has a paired landscape site that is upslope from the trail and intended to represent the conditions that would have existed without the presence of the trail. Paired locations were determined based on field inspections. The location of every site was surveyed using a Geode GN3S receiver with ~5 cm accuracy. The final dataset includes 106 sampling locations, including 60 paired locations (30 trail and 30 landscape) and 46 unpaired landscape locations in Regions B and C (Figure 2).

2.5 Laboratory Analysis of Soils

At each trail and paired landscape location, soil samples were extracted in the top ~5 cm of the soil column and tested in the laboratory for sand, silt, and clay fractions, organic matter, and dry density. For each location, these characteristics were determined by combining three soil

samples collected within approximately 1 m of the sampling location. Each sample was approximately 150 g. USDA sand, silt, and clay fractions were obtained via sieve and hydrometer analysis in accordance with ASTM D6913 and ASTM D7928, respectively (ASTM International, 2017; ASTM International, 2021). A ~50 g sub-sample was also used to measure organic content in accordance with ASTM D2974, Method A (ASTM International, 2020). The dry density was measured using the in-situ sand cone method in accordance with the ASTM D1556 (ASTM, 2016).

2.6 Soil Moisture Sampling

Soil moisture sampling was conducted at Maxwell Ranch during the spring and summer of 2023 to avoid snow and frozen ground that can occur in winter. Within the study period, the sampling dates were selected to observe the widest possible range of moisture conditions on the ranch. A CoAgMET weather station (Station ID 058690) is located about 0.5 km north of the ranch (at 40.9656°N, 105.2186°W) and records daily precipitation data. Figure 3 shows the precipitation during the study period along with the sampling dates. Sampling occurred on six dates including: 09 May 2023, 01 June 2023, 14 June 2023, 09 July 2023, 25 July 2023, and 12 September 2023. Increasingly wet conditions occurred until mid-July followed by a gradual dry-down during the remainder of the study period.

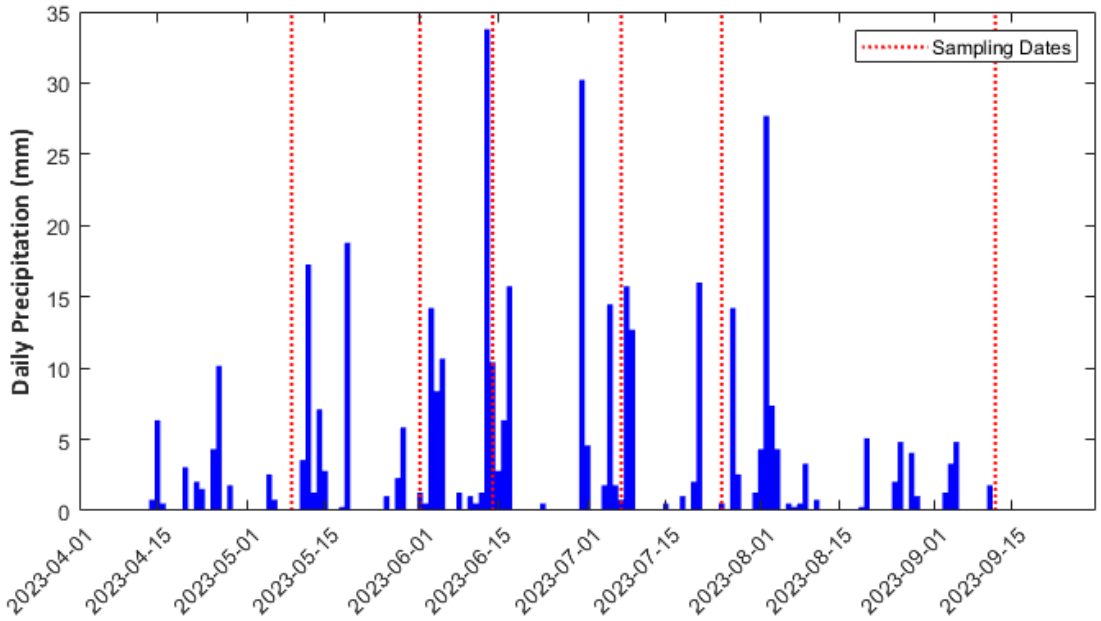

Figure 3. Daily precipitation recorded at the Virginia Dale CoAgMet weather station (Station ID 058690) near Maxwell Ranch along with soil moisture sampling dates.

Volumetric soil moisture was measured in the top 5 cm of the soil using a Stevens HydraGo portable HydraProbe. This device uses coaxial impedance dielectric reflectometry to measure soil moisture and has an accuracy of ± 0.01 to 0.03 cm^3/cm^3, depending on the soil type (Stevens Water, 2018). Three measurements were made within approximately 1 m of each sampling location and averaged to determine the soil moisture of the sampling location. The HydraProbe could not be inserted into the trails due to their compaction. Thus, soil samples of approximately 80 g were extracted at the trail and paired landscape sites in the top ~5 cm of the soil to quantify gravimetric soil moisture via the ASTM D2216 oven dry method (ASTM, 2019). The dry density was then used to convert the gravimetric water content to the volumetric water content. At the paired landscape locations, these volumetric water contents were compared to the HydraProbe measurements remove any bias in the gravimetric measurements and ensure consistency between the different measurement methods.

2.7 EMT+VS Model Inputs

Coarse resolution soil moisture for each date was obtained at a 9 km resolution from the SMAP Level 3 passive enhanced product via the Earthdata portal (O'Neill et al., 2021). Two of the six sampling dates did not have a Level 3 product available, so a product from an adjacent day was used. This SMAP product was selected because Fischer (2024) showed that it accurately estimates the spatial average soil moisture across Maxwell Ranch. The product for 15:00 to 18:00 UTC was used as this timeframe most closely aligns with the fieldwork. A single SMAP grid cell captures the entirety of Maxwell Ranch. The fine resolution topographic attributes were calculated by Fischer (2024) based on a 10-m DEM from the Natural Resources Conservation Service. Fractional vegetation cover was estimated as the enhanced vegetation index (EVI), which is based on the red, blue, and near-infrared reflectance. EVI was used because Fischer (2024) showed that this vegetation index produces the best soil moisture estimates among the vegetation indices tested. EVI can only be obtained when the sky is clear, so the EVI from August 9th was applied for all sampling dates. This date was selected because its EVI had the highest Pearson correlation coefficient (r = 0.81) with soil moisture among the available dates. The binary raster identifying trail locations was developed by digitizing trail locations based on satellite imagery in Google Earth (Google, 2022).

2.8 EMT+VS Model Application

The EMT+VS model was run for four scenarios. In the first scenario, the pre-existing EMT+VS model (without trail adjustments) was applied to Maxwell Ranch. In particular, the model parameters were calibrated using the undisturbed landscape locations in Regions B and C as well as the paired landscape locations. Then, the performance is investigated not only for these landscape points but also the trail points. When calibrating this scenario, the thickness of

the hydrologically active layer (δ_0) was set at the measurement depth (5 cm), which is consistent with prior applications of the EMT+VS model (Pauly et al., 2020; Ranney et al., 2015). The remaining parameters were calibrated within the feasible ranges previously used at Maxwell Ranch by Fischer (2024). The parameter values were selected to maximize the Nash-Sutcliffe Coefficient Efficiency (NSCE) when combining all dates together (i.e., the space-time NSCE) (Nash and Sutcliffe, 1970). The space-time NSCE has a value of one when the observations are perfectly reproduced and lower values (even below zero) as errors increase. Using the space-time average soil moisture as a model would produce a value of zero. Thus, values above zero indicate viable models.

In the second scenario, the vegetation adjustment was allowed for the trail locations. In this scenario, all the parameters associated with undisturbed locations were kept at the values obtained in the first scenario. The vegetation adjustment parameter ζ_T was calibrated to maximize the space-time NSCE for the trail points, so the strength of the trail adjustment is determined by the calibration.

In the third scenario, the porosity adjustment was allowed for the trail locations (the vegetation adjustment was not included). Again, all parameters were kept at the values of the first scenario except the porosity adjustment parameter ρ_T, which was calibrated to maximize the space-time NSCE for the trail points.

In the fourth scenario, both the vegetation and porosity adjustments were allowed for the trail locations. Again, all parameters were kept at the values of the first scenario except the vegetation adjustment parameter ζ_T and the porosity adjustment parameter ρ_T, which were calibrated to maximize the space-time NSCE for the trail points.

3 RESULTS

3.1 Observed Topography and Vegetation

Figure 4 shows the histograms of the topographic and vegetation characteristics across all the trail and paired landscape sampling locations. The topographic characteristics evaluated here are the most important ones in the EMT+VS model including elevation, log of specific contributing area, slope, and the cosine of aspect. The last two characteristics affect the potential solar radiation index. Curvature is used to predict soil depth but has little effect on the model results. The distributions show that characteristics at trail sampling locations are generally similar to those at the paired landscape locations. However, the log of contributing area is higher on average for trails than paired landscape locations (because the paired landscape locations are upslope of the trails).

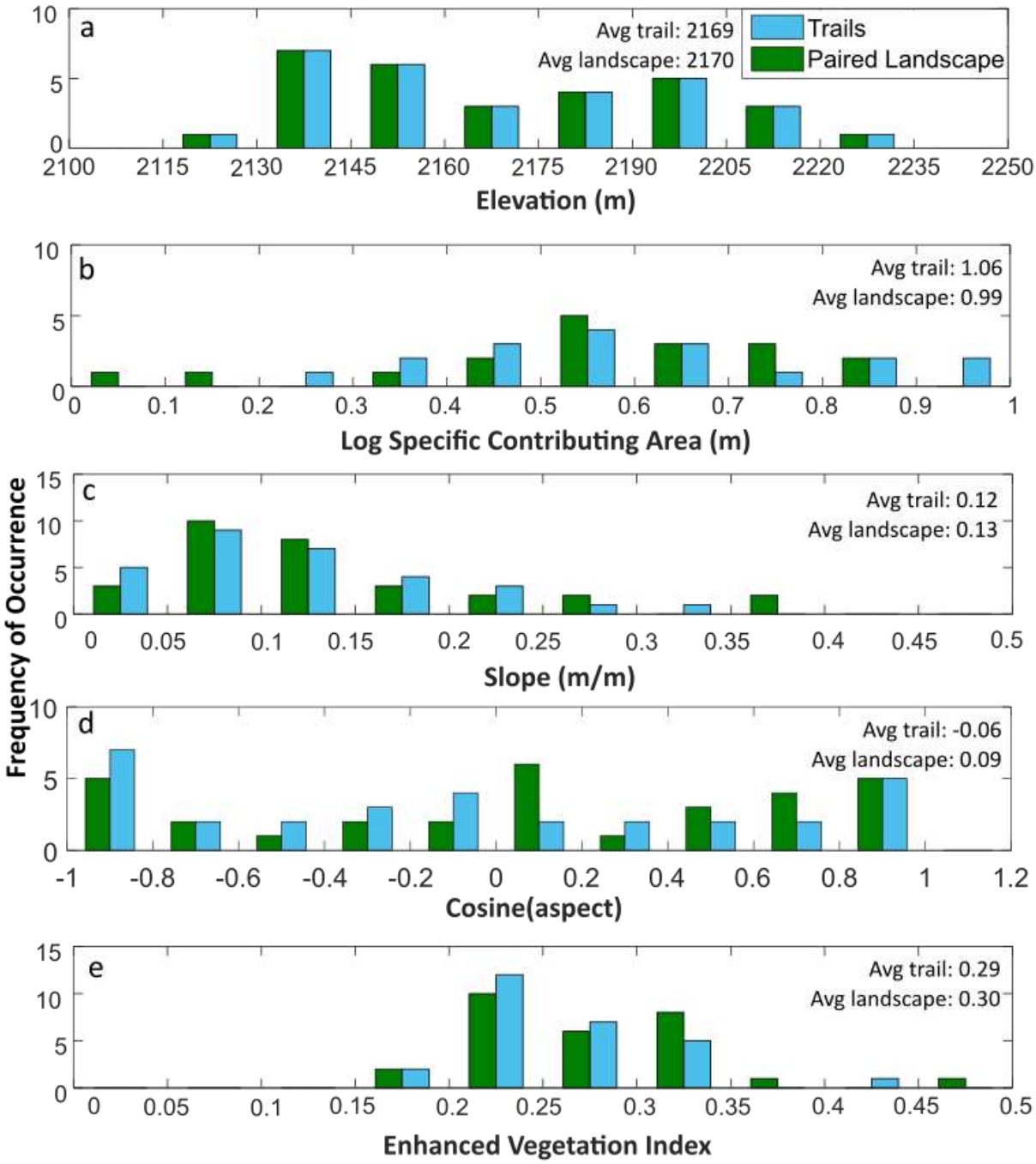

Figure 4. Histograms of (a) elevation, (b) log of specific contributing area, (b) slope, (c) cosine of aspect, and (d) enhanced vegetation index for all locations within the SMAP grid cell, all trail locations, and the trail sampling locations.

3.2 Observed Soil Compositions

Figure 5 shows histograms for the fractions of sand, silt, clay, and organic matter across the paired trail and landscape sampling locations. Overall, sand is the dominant particle size, followed by silt. The trail locations typically have lower silt content and greater sand content than the paired landscape locations. On average, the silt fraction is 0.11 lower at trail sites than landscape sites. On average, the sand fraction is 0.12 higher at trail sites than landscape sites. The reduction in silt for trail locations may occur because trails have less vegetation cover, which exposes the surface to greater wind and water erosion (removing the easier-to-transport silt particles). For a different field site in the Front Range of Colorado, Ranney et al. (2015) also observed less silt at locations where vegetation cover is thinner. The higher sand fraction is partially a consequence of the lower fraction of silt because the sand, silt, and clay fractions sum to one. Organic matter is also slightly lower (0.001) for trail locations than landscape locations, which is expected from the lower vegetation cover on trails.

Figure 5e directly compares the sand, silt, clay, and organic matter values for individual pairings of landscape and trail points. For the sand, silt, and clay fractions, the correlations between the paired trail and landscape values are 0.52, 0.55, and 0.43, respectively. These values suggest that a higher fraction of sand, silt, or clay at a landscape point has some association with a higher value at the associated trail point, but substantial random differences also occur. For the organic matter, the correlation between the paired trail and landscape locations is 0.05, which suggests almost no association between the landscape and trail conditions.

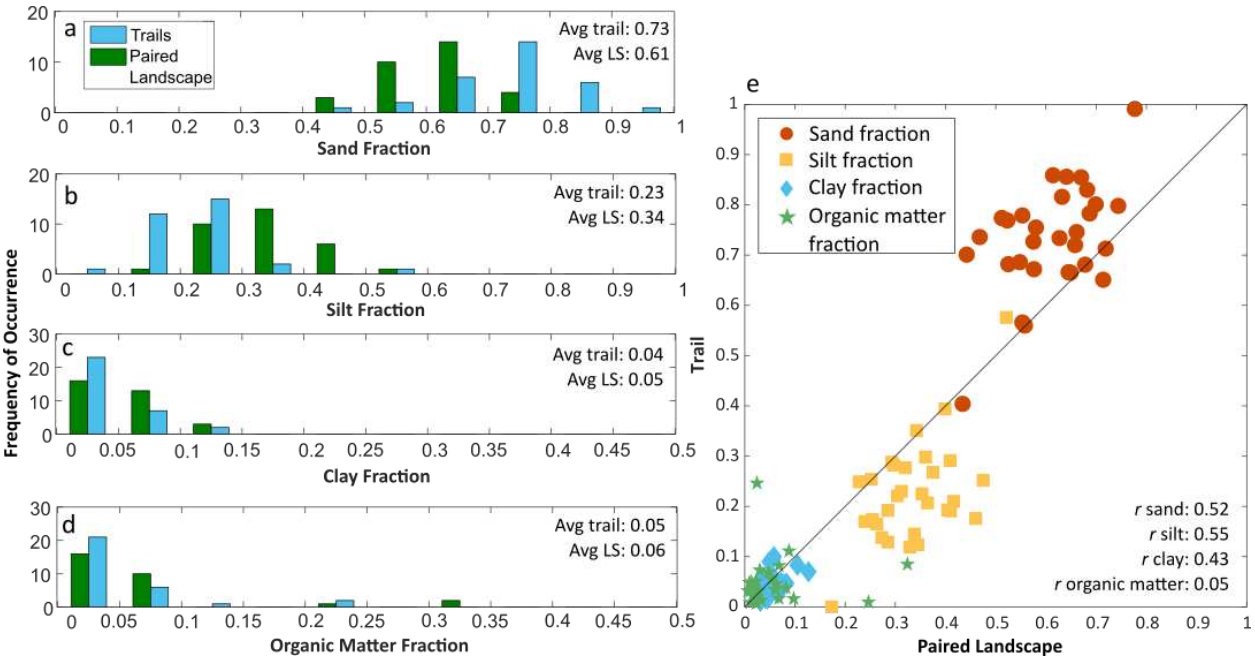

Figure 5. Histograms of the (a) sand, (b) silt, (c) clay, and (d) organic matter fractions for paired landscape and trail sampling locations. (e) Comparisons of the sand, silt, clay, and organic matter fractions for individual pairs of trail and landscape locations. LS denotes landscape, and r denotes correlation coefficient.

3.3 Observed Porosity

Figure 6a shows the histograms of porosity for the paired trail and landscape locations. The porosity values for the landscape locations are highly variable, exhibiting a total range of 0.89. Although high porosity values can occur in highly organic soils (Rezanezhad et al., 2016), the porosities near one and close to zero in Figure 6a are likely due to measurement errors. The porosity values for the trail locations are much less variable (the range is 0.36). The smaller range could suggest that vehicle traffic has a homogenizing influence on porosity and/or that measurement errors are lower for trails. The primary source of measurement error in the porosity values is the estimation of the excavated volume in the sand cone method (which is used to determine the dry density). On average, the porosity at the trail sites is 0.05 lower than at the landscape sites or 86% of the porosity of the paired landscape sites. The lower porosity is expected because vehicle traffic compacts the soil matrix. The small difference in the average

porosities of the trail and landscape locations is likely due to the coarse-grained soil. Figure 6b compares the porosities for the individual pairings of trail and landscape locations. The correlation coefficient $r = 0.43$ suggests that the landscape porosity has only a weak association with the adjacent trail porosity.

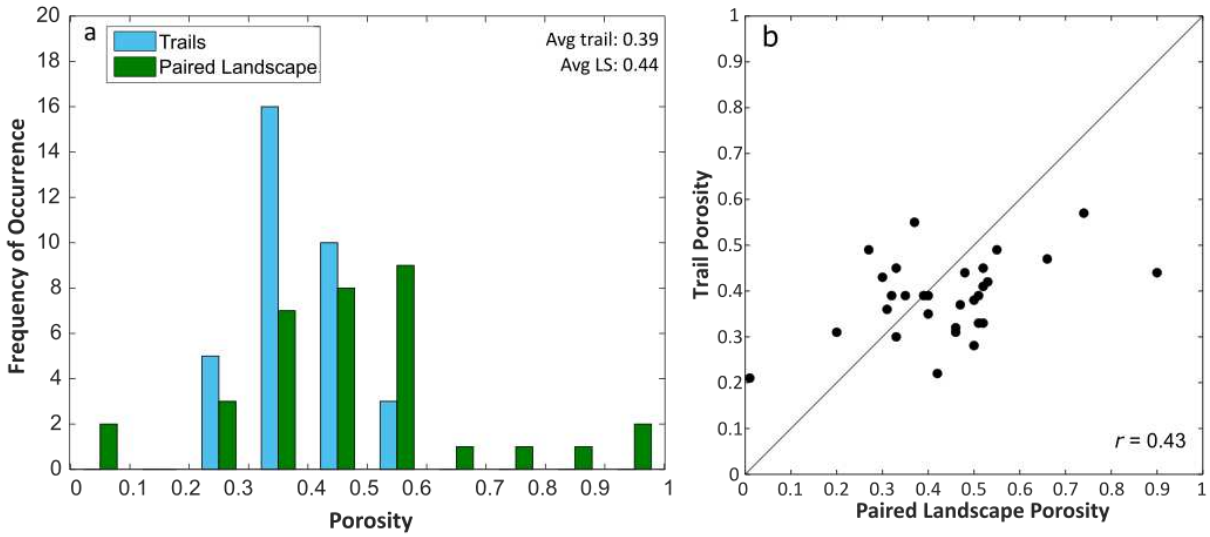

Figure 6. (a) Histograms of porosity for paired landscape and trail sampling locations and (b) comparison of porosities for individual pairings of landscape and trail locations. LS denotes landscape, and r denotes correlation coefficient.

3.4 Observed Soil Moisture

Figure 7 shows maps of the observed soil moisture values for the unpaired landscape locations in Regions B and C and the paired trail and landscape locations. For the paired locations, each inner circle indicates the trail soil moisture, and each outer circle indicates the paired landscape soil moisture. The paired landscape soil moisture shown in these maps is from the HydraProbe. The first two dates have moderate soil moisture, the middle two dates have high soil moisture (with June 14 being the wettest date), and the last two dates have low soil moisture (with July 25 being the driest date). Overall, locations in the valley bottoms tend to have wet conditions for all sampling dates, while the other locations vary between dates.

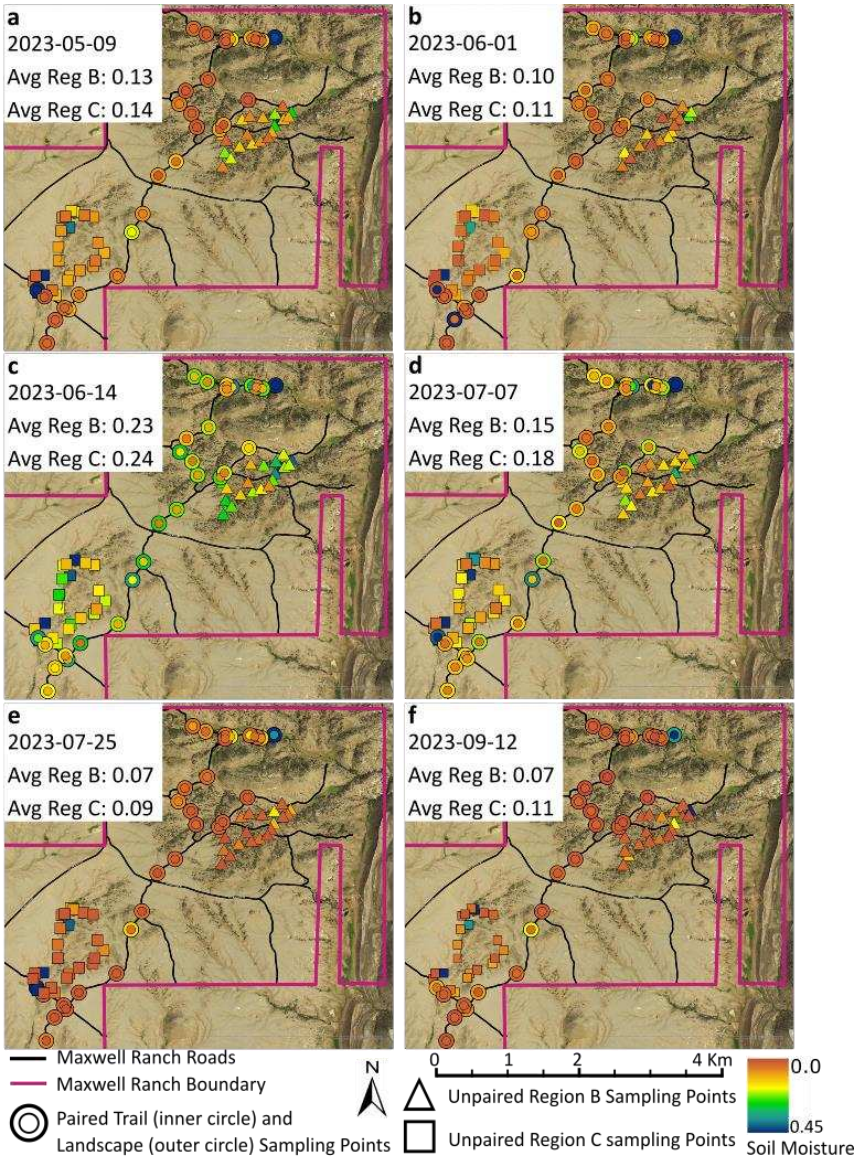

Figure 7. Volumetric soil moisture values derived from oven drying at paired trail points as well as volumetric soil moisture values from HydraProbe measurements at paired landscape points and unpaired landscape points in Regions B and C for all sampling dates. The reported averages are from the HydraProbe observations for Regions B and C.

Figure 8a-8f shows the histograms of observed soil moisture (volumetric water content) at paired trail and landscape locations for the six sampling dates. Overall, the soil moisture is lower for the trail locations than the landscape locations, and the largest difference is observed for 2023-06-14, which is the wettest date. Considering all dates, the soil moisture of the trail locations is 0.02 cm^3/cm^3 smaller than (or 88% of) the soil moisture of the paired landscape

locations when the paired landscape soil moisture derived from the oven drying method. The average ratio of the trail and paired landscape soil moisture is 0.72, 1.47, 0.77, 0.77, 0.63 and 0.89 for the six sampling dates using the oven drying data. When the HydraProbe soil moisture is used for the landscape locations, the trail soil moisture is on average 0.04 cm^3/cm^3 smaller than (or 73% of) the paired landscape soil moisture. The average ratio of the trail and paired landscape soil moisture is 0.68, 0.77, 0.57, 0.69, 0.64, and 1.04 for the six sampling dates using the HydraProbe data.

Figure 8g compares the soil moisture (volumetric water content) at individual pairs of trail and landscape locations using data from the oven drying method for the landscape locations. Figure 8h makes the same comparison using the HydraProbe data for the landscape locations. Higher correlations are typically observed between the soil moisture at the paired trail and landscape locations on drier dates. For example, using the soil moisture derived from the oven drying method, r is 0.81 and 0.87 for July 25th and September 9th, respectively (the two driest dates). In contrast, r is 0.38 and 0.45 on June 14th and July 7th, respectively (the two wettest dates) using the soil moisture derived from gravimetric measurements. When using the HydraProbe data, the correlations are still typically higher for the drier dates, but the correlations are more inconsistent.

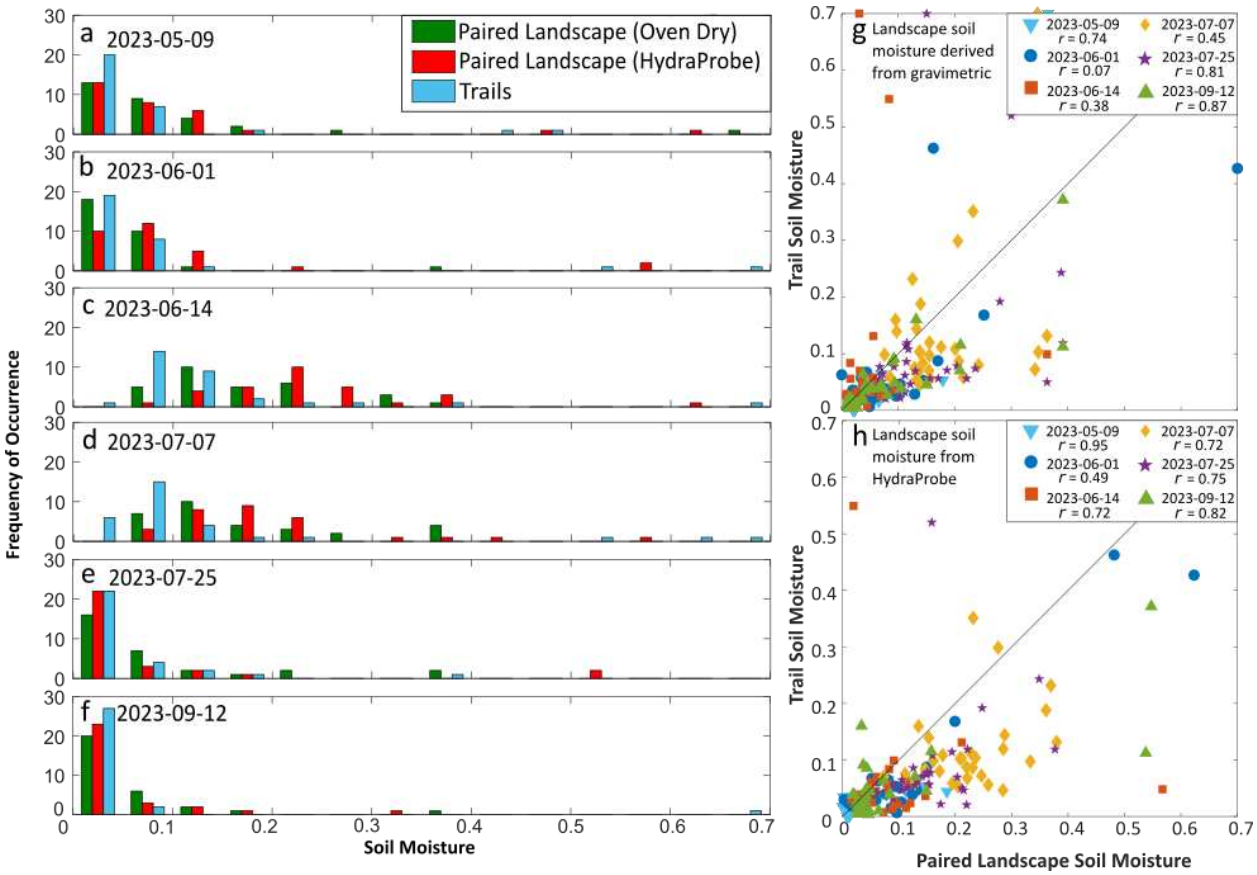

Figure 8. Histograms of soil moisture for paired trail and landscape locations on (a) 2023-05-09, (b) 2023-06-01, (c) 2023-06-14, (d) 2023-07-07, (e) 2023-07-25, and (f) 2023-09-12. Comparisons of the soil moisture at individual pairings of trail and landscape locations (g) derived from oven drying and (h) from the HydraProbe.

3.5 EMT+VS Model Results

The calibrated parameter set for each EMT+VS model scenario is shown in Table 1. For Scenario 2, the vegetation adjustment parameter is calibrated to 0.78, which indicates that the original fractional vegetation cover in trail cells is multiplied by 78% to estimate the vegetation cover on the trails. Although no field measurements of vegetation cover were collected, visual inspections indicate that almost no vegetation cover occurs in the wheel tracks of the trails. Thus, this calibrated value likely overestimates the extent of trail vegetation cover. In Scenario 3, the porosity adjustment was calibrated to a value of 0.83 (the trail porosity is 83% of the landscape porosity). This number is very close to the 86% that was observed from the field

measurements. In Scenario 4, both the vegetation and porosity adjustments were allowed, and they each calibrated to 0.86 and 0.90, respectively.

Table 1. Calibration limits and calibrated parameter values for each EMT+VS model scenario

Parameter	Calibration Limits		Calibrated Parameters for Model Scenarios			
	Lower	Upper	1. Non-Adjusted	2. Veg. Trail Adjustment	3. Porosity Trail Adjustment	4. Veg. & Porosity Trail Adjustments
Porosity ϕ	0.20	0.45	0.45	0.45	0.45	0.45
Horizontal pore disconnectedness γ_h	1.00	36.0	1.00	1.00	1.00	1.00
Vertical pore disconnectedness γ_v	6.00	36.0	35.1	35.1	35.1	35.1
Radiative ET exponent β_r	0.10	5.00	1.77	1.77	1.77	1.77
Aerodynamic ET exponent β_a	0.10	5.00	0.10	0.10	0.10	0.10
Priestly-Taylor coef. minus one α	0.10	0.40	0.18	0.18	0.18	0.18
Relation of hydraulic to topographic gradient ϵ	0.10	3.00	1.46	1.46	1.46	1.46
Portion of soil from transpiration layer η	0.00	1.00	0.01	0.01	0.01	0.01
Vertical saturated hydraulic conductivity K_s	1.00	7000	2725	2725	2725	2725
Anisotropy of sat. hydraulic conductivity ι	1.00	700	700	700	700	700
Minimum topographic curvature with soil κ_0	-9999	-0.36	-3203	-3203	-3203	-3203
Interception efficiency λ	0.00	1.00	1.00	1.00	1.00	1.00
Shading effect on soil evaporation μ	1.00	10.0	4.52	4.52	4.52	4.52
Potential evapotranspiration (PET) $\overline{E_p}$	3.00	8.00	3.00	3.00	3.00	3.00
PET elevation dependence ω	-0.0015	0.0015	0.00	0.00	0.00	0.00
Vegetation adjustment factor for porosity χ	0.00	0.50	0.14	0.14	0.14	0.14
Trail vegetation multiplier ζ_T	0.00	1.00	N/A	0.78	N/A	0.86
Trail porosity multiplier ρ_T	0.00	1.00	N/A	N/A	0.83	0.90

Figure 9 shows the soil moisture patterns produced by the EMT+VS model for the four scenarios. The non-adjusted model (Figure 9a and 9b) estimates slightly drier conditions on the trails than nearby landscape locations, but the difference between the trail and landscape moisture values is subtle. In the non-adjusted model, vegetation increases the porosity ($\chi > 0$) and shades the surface ($\mu > 1$), which reduces soil evaporation. Both effects increase soil moisture where vegetation is thicker. Because trail cells tend to have lower vegetation cover than undisturbed landscape cells, they tend to be drier. In Scenario 2, the vegetation cover of trail cells is further reduced, which promotes even drier conditions in those cells. In Scenario 3,

the porosity of trail cells is reduced, which also promotes drier conditions. Lower porosity produces drier conditions because the hydraulic conductivity is calculated as a function of the soil moisture divided by the porosity. If the porosity is lower, a lower soil moisture is sufficient for the outflows from the soil to balance the infiltration. In Scenario 4, the trails are drier than Scenario 1 again, but less so than in Scenario 3.

Figure 10 compares the observed and estimated soil moisture values at the trails for the four model scenarios. For Scenario 1, the model typically overestimates the observed soil moisture values at the trails. This result occurs because this scenario was calibrated using only the landscape locations, and the field observations show that trails tend to be drier than landscape locations. For Scenarios 2 and 3, somewhat better agreement is observed between the observations and model at the trails because the model includes calibrated adjustments to reproduce the trail moisture conditions. Scenario 4 shows similar agreement with the field observations as Scenarios 2 and 3. All four scenarios show substantial scatter around the 1:1 line, which suggests that the soil moisture estimates for the trails include noteworthy errors.

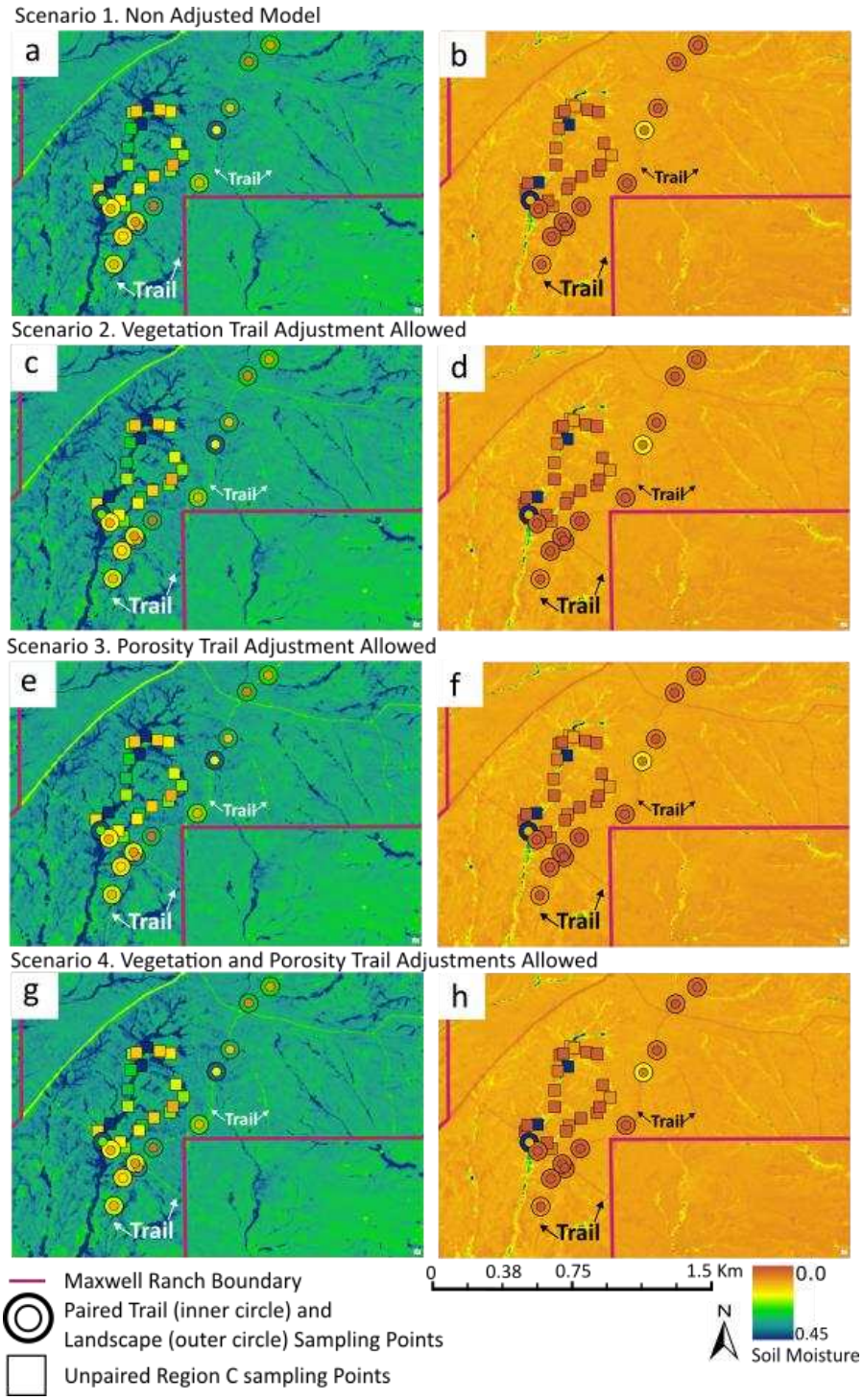

Figure 9. Fine resolution soil moisture maps produced by the EMT+VS model for the wettest sampling date (2023-06-14; left side of figure) and driest sampling date (2023-07-25; right side of figure). Parts (a and b) show the non-adjusted EMT+VS model, (c and d) show the model with the vegetation trail adjustment, (e and f) show the model with the porosity trail adjustment, and (g and h) show the model with both vegetation and porosity adjustments.

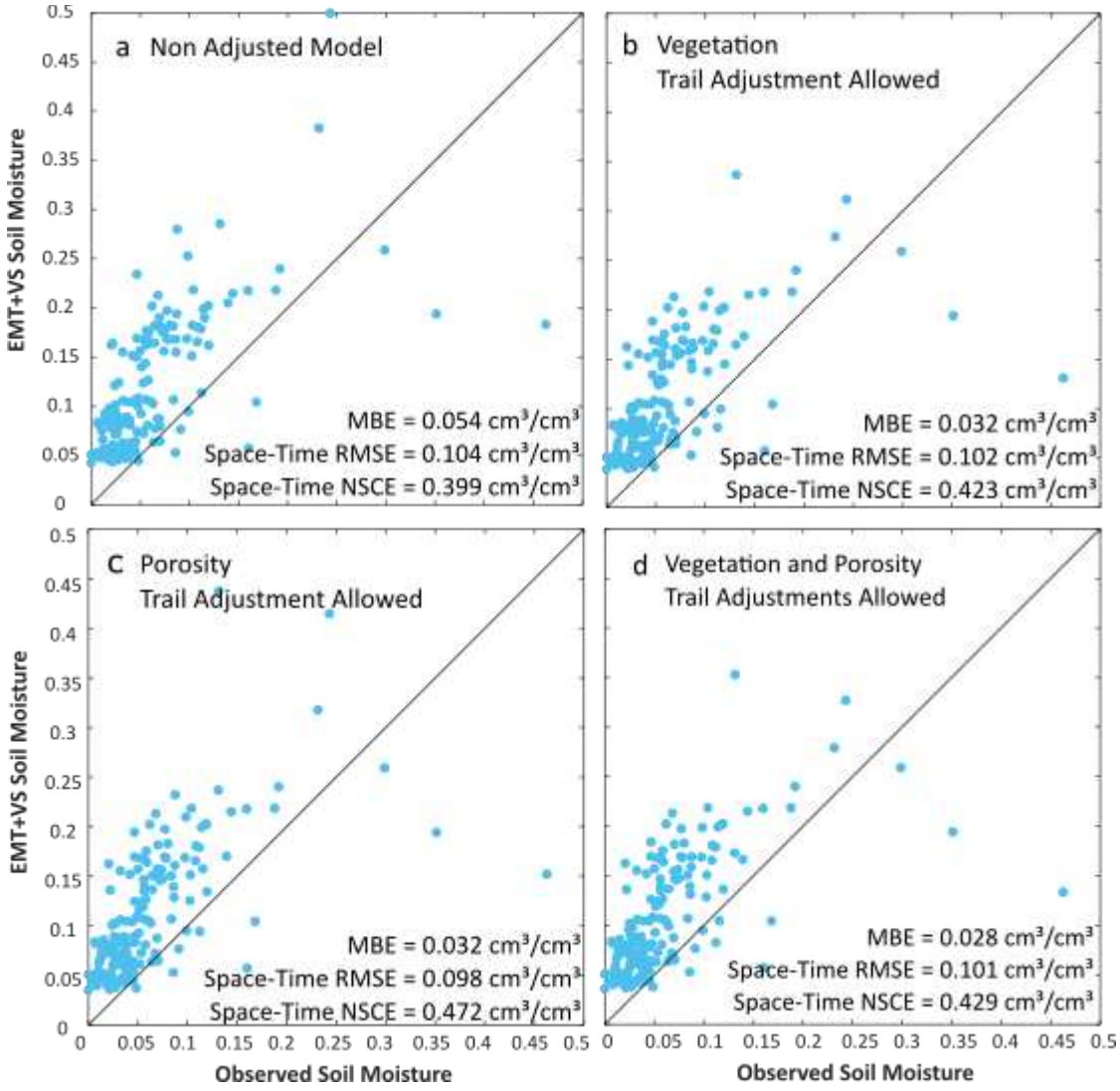

Figure 10. Comparison of field observations and EMT+VS estimates of trail soil moisture for (a) the non-adjusted model, (b) the model with the vegetation trail adjustment, (c) the model with theu porosity trail adjustment, and (d) the model that allows both vegetation and trail adjustments.

The accuracy of each model was evaluated using the mean bias error (MBE), root mean squared error (RMSE), average spatial NSCE, and space-time NSCE (Table 2). The average spatial NSCE examines how well spatial variability is reproduced by the downscaling model, while the space-time NSCE examines how well both spatial and temporal variations are reproduced. The MBE for the non-adjusted model at landscape and trail locations was 0.018 cm^3/cm^3 and 0.054 cm^3/cm^3, respectively, which indicate overestimation of the soil moisture,

with higher overestimation at trail locations. For the non-adjusted model, the RMSE is 0.080 cm^3/cm^3 for landscape locations. This RMSE is larger than the RMSE reported by Fischer (2024) when they considered four regions with undisturbed landscape locations and soil moisture observations from 2022 (their RMSE was 0.066 cm^3/cm^3). The lower performance seen here could occur because the conditions were much wetter and diverse in 2023 than 2022. It could also occur because a late summer EVI image had to be used due to spring cloud cover, and Fischer (2024) found that using a spring image improves performance. For the non-adjusted model, the RMSE at the trail locations (0.104 cm^3/cm^3) is higher than the landscape locations.

For Scenarios 2, 3, and 4, the MBE at trail locations is reduced to 0.032, 0.032, and 0.028 cm^3/cm^3, respectively. This indicates that the trail adjustments allow the model to better predict the soil moisture at the trails. The MBE at landscape locations remains static because trail adjustments were not applied to those locations. The space-time RMSE at the landscape locations is also unchanged because the trail adjustments do not apply to landscape locations and all other parameters remain unchanged from Scenario 1. Small improvements in RMSE are observed for the trail locations for Scenarios 2, 3, and 4 compared to the non-adjusted model in Scenario 1. The average spatial NSCE remains nearly the same on trails when comparing Scenario 1 to Scenarios 2 and 4, but greater improvement is observed for Scenario 3. However, the space-time NSCE shows more substantial improvements for the trails when comparing the trail adjusted scenarios to the non-adjusted model. Thus, even though considerable errors remain for the trails in Scenarios 2, 3, and 4, more space-time variation is explained when the trail adjustments are included.

Table 2. Performance statistics for four EMT+VS model scenarios at the landscape locations in Regions B and C and the trail locations

Scenario	MBE (cm^3/cm^3)		RMSE (cm^3/cm^3)		Average Spatial NSCE (cm^3/cm^3)		Space-Time NSCE (cm^3/cm^3)	
	B and C	**Trails**	**B and C**	**Trails**	**B and C**	**Trails**	**B and C**	**Trails**
1. Non-adjusted model	0.018	0.054	0.080	0.104	0.650	0.444	0.697	0.399
2. Vegetation adjustment	0.018	0.032	0.080	0.102	0.650	0.442	0.697	0.423
3. Porosity adjustment	0.018	0.032	0.080	0.098	0.650	0.506	0.697	0.472
4. Veg. and Por. adjustments	0.018	0.028	0.080	0.101	0.650	0.443	0.697	0.429

4 DISCUSSION

Previous studies have shown that vehicle traffic reduces vegetation cover and porosity on trails. However, as shown in Figure 1, the net effect of these alterations on the soil moisture of trails is unclear (they could lead to higher or lower soil moisture). In this study, field measurements show that trail locations typically have lower soil moisture than paired landscape locations. These results suggest that the combined effects of greater wind exposure, reduced shading, and lower infiltration (all of which reduce the soil moisture) are stronger than the combined effects of reduced interception, reduced root-water uptake, and reduced drainage (all of which increase soil moisture). Furthermore, the model produced drier conditions when either the vegetation or the porosity was reduced. When vegetation is reduced in the model, the effect of less shading outweighs the effects of less interception and less root-water uptake (wind exposure is not represented in the model). Vegetation also affects the porosity in the EMT+VS model. When porosity is reduced, the reduction in drainage produces drier soil moisture conditions because infiltration is not related to the porosity. These observations and model results consider primarily herbaceous vegetation, coarse-grained soils, and traffic by relatively lightweight vehicles (pickup trucks). Different results could occur in different settings.

5 CONCLUSIONS

In this study, the EMT+VS soil moisture downscaling model was generalized to explicitly consider the soil moisture of vehicle trails. Specifically, methods were included that can reduce the vegetation cover and porosity for known trail locations. The model was tested by application to the Maxwell Ranch study region, which has been previously used to test soil moisture downscaling and soil strength models for undisturbed landscape locations. The region is semiarid and has coarse-grained soils. Maxwell Ranch also includes ~46 km of well-developed trails. Porosity and soil moisture were measured at 30 paired trail and landscape locations, which were selected to have diverse topographic and vegetation conditions. For the conditions considered in this study, the following conclusions can be made:

1. Based on field observations, the trails have less silt and more sand than the paired landscape locations. Trails may have less silt because their reduced vegetation cover exposes the surface to wind and water erosion. This exposure may preferentially remove silt particles because they are easier to transport than sand. Less silt was also observed for a nearby study region for undisturbed locations that had less vegetation cover (Ranney et al., 2015).
2. The trail locations have lower observed porosities than the paired landscape locations. On average, the porosity of the trail locations is 86% of the paired landscape locations. The lower porosities likely occur due to the compaction of the trails by vehicle traffic. The porosities of the trail and landscape points are relatively similar because the soils in the study region are coarse-grained and usually dry and are thus strong under compression (Bullock, 2023).

3. Trails in the study region typically have lower observed soil moisture than the paired landscape locations. Specifically, the trails on average have 73-88% of the moisture of the paired landscape locations. The lower soil moisture can be explained by the lower porosities, which increase drainage on the trails. The lower soil moisture can also be explained by the visibly lower vegetation cover of the trails, which allows more insolation and therefore more soil evaporation than the landscape locations. Other phenomena might also contribute to the drier soil conditions of trails.
4. When vegetation and porosity trail adjustments are included in the EMT+VS model, EMT+VS more accurately explains the soil moisture of the trail locations than a non-adjusted model that is calibrated to only undisturbed landscape locations. The trail adjustments also produce trails that are drier than the adjacent landscape, which is consistent with the field observations. The calibrated vegetation adjustment produces higher vegetation cover than visual inspection suggests, while the calibrated porosity adjustment is similar to the field observations. Even with the vegetation and porosity adjustments, the errors are higher at the trail locations than the landscape locations. This result suggests that the machine-ground interaction increases the uncertainty of the soil moisture estimates for trails relative to the undisturbed landscape.

The results of this study are expected to apply only to regions with similar conditions to the study region. Future research should test the applicability of the trail adjustments for regions with wetter climates and/or fine-grained soils. This study did not consider trail locations with engineered materials, culverts, rutting from vehicles, or rilling from erosion. Microtopography of trails is expected to change their soil moisture. The results of this study may also depend on size of the trails relative to the EMT+VS model resolution, which was 10 m in this study. As the

resolution of remote sensing data becomes finer, the vegetation cover of the trails is expected to be captured more accurately. Thus, vegetation adjustment on trails may become less necessary. Trails generated by heavier vehicles (farm or military equipment) should also be considered. Additionally, future research should test the abilities of automatically detecting trails for modeling trail adjustments. The implications of this study on the strength of trail soils should also be considered. More accurate soil moisture estimates on trails will improve soil strength estimates, but the magnitude of the improvement is unclear. Finally, the implications for vehicle mobility and routing across the landscape could also be studied.

REFERENCES

Ahmad, S., Kalra, A., & Stephen, H. (2010). Estimating soil moisture using remote sensing data: A machine learning approach. Advances in water resources, 33(1), 69-80. https://doi.org/10.1016/j.advwatres.2009.10.008.

Alemohammad, S. H., Kolassa, J., Prigent, C., Aires, F., & Gentine, P. (2018). Global downscaling of remotely sensed soil moisture using neural networks. Hydrology and Earth System Sciences, 22(10), 5341-5356. https://doi.org/10.5194/hess-22-5341-2018

ASTM International. (2017). *Standard Test Methods for Particle-Size Distribution (Gradation) of Soils Using Sieve Analysis* (ASTM D6913/D6913M-17). Retrieved from https://www.astm.org.

ASTM International. (2020). *Standard Test Methods for Determining the Water (Moisture) Content, Ash Content, and Organic Material of Peat and Other Organic Soils* (ASTM D2974-20e1). Retrieved from https://www.astm.org.

ASTM International. (2021). *Standard Test Methods for Particle-Size Distribution (Gradation) of Soils Using the Sedimentation (Hydrometer) Analysis* (ASTM D7928-21). Retrieved from https://www.astm.org.

Bindlish, R., Jackson, T., Cosh, M., Sun, R., Yueh, S., & Dinardo, S. (2008, July). Combined passive and active soil moisture observations during clasic. In *IGARSS 2008-2008 IEEE International Geoscience and Remote Sensing Symposium* (Vol. 2, pp. II-237). IEEE. https://doi.org/10.1109/IGARSS.2008.4778971

Botta, G. F., Becerra, A. T., & Tourn, F. B. (2009). Effect of the number of tractor passes on soil rut depth and compaction in two tillage regimes. Soil and Tillage Research, 103(2), 381-386. https://doi.org/10.1016/j.still.2008.12.002

Bullock, M. D. (2023). Predicting Unsaturated Soil Strength for Mobility Assessments. Master's Thesis, Colorado State University, Fort Collins, CO.

Campbell, G. S. (1974). A simple method for determining unsaturated conductivity from moisture retention data. *Soil science, 117(6)*, 311-314. http://dx.doi.org/10.1097/00010694-197406000-00001

Coleman, M. L., & Niemann, J. D. (2013). Controls on topographic dependence and temporal instability in catchment-scale soil moisture patterns. *Water Resources Research*, *49*(3), 1625-1642. https://doi.org/10.1002/wrcr.20159

Colliander, A., Reichle, R. H., Crow, W. T., Cosh, M. H., Chen, F., Chan, S., ... & Yueh, S. H. (2021). Validation of soil moisture data products from the NASA SMAP mission. IEEE Journal of selected topics in applied earth observations and remote sensing, 15, 364-392. https://doi.org/10.1109/JSTARS.2021.3124743

Cowley, G. S., Niemann, J. D., Green, T. R., Seyfried, M. S., Jones, A. S., & Grazaitis, P. J. (2017). Impacts of precipitation and potential evapotranspiration patterns on downscaling soil moisture in regions with large topographic relief. Water Resources Research, 53(2), 1553-1574. https://doi.org/10.1002/2016WR019907

Deshon, J. P., Niemann, J. D., Green, T. R., Jones, A. S., & Grazaitis, P. J. (2020). Stochastic analysis and probabilistic downscaling of soil moisture in small catchments. Journal of Hydrology, 585, 124711. https://doi.org/10.1016/j.jhydrol.2020.124711

Dobriyal, P., Qureshi, A., Badola, R., & Hussain, S. A. (2012). A review of the methods available for estimating soil moisture and its implications for water resource management. Journal of Hydrology, 458, 110-117. https://doi.org/10.1016/j.jhydrol.2012.06.021

Eylander, J., Bieszczad, J., Ueckermann, M., Peters, J., Brooks, C., Audette, W., & Ekegren, M. (2023). Geospatial Weather Affected Terrain Conditions and Hazards (GeoWATCH) description and evaluation. *Environmental Modelling & Software*, *160*, 105606. https://doi.org/10.1016/j.envsoft.2022.105606

Fang, B., Lakshmi, V., Bindlish, R., Jackson, T. J., Cosh, M., & Basara, J. (2013). Passive microwave soil moisture downscaling using vegetation index and skin surface temperature. *Vadose Zone Journal*, *12*(3). https://doi.org/10.2136/vzj2013.05.0089

Fischer, S. C., 2024. Assessing the influence of model inputs on performance of the EMT+VS soil moisture downscaling model for a large foothills region in northern Colorado. Master's Thesis, Colorado State University, Fort Collins, CO.

Google. (2022). Maxwell Ranch [Google Earth version]. Retrieved from http://www.google.com/earth/index.html [April 2022].

Grieco, N. R., Niemann, J. D., Green, T. R., Jones, A. S., & Grazaitis, P. J. (2018). Hydrologic downscaling of soil moisture using global data sets without site-specific calibration. *Journal of Hydrologic Engineering*, *23*(11), 04018048. https://doi.org/10.1061/(ASCE)HE.1943-5584.0001702

Hansson, L., Šimůnek, J., Ring, E., Bishop, K., & Gärdenäs, A. I. (2019). Soil compaction effects on root-zone hydrology and vegetation in boreal forest clearcuts. Soil Science Society of America Journal, 83, S105-S115. https://doi.org/10.2136/sssaj2018.08.0302

Heathwaite, A., Quinn, P. F., & Hewett, C. (2005). Modeling and managing critical source areas of diffuse pollution from agricultural land using flow connectivity simulation. Journal of Hydrology, 304, 446-461. https://doi.org/10.1016/j.jhydrol.2004.07.043

Heštera, H., & Pahernik, M. (2018). Physical-geographic factors of terrain trafficability of military vehicles according to Western World methodologies. Croatian Geographical Bulletin, 80(2). https://doi.org/10.21861/HGG.2018.80.02.01

Hoehn, D. C., Niemann, J. D., Green, T. R., Jones, A. S., & Grazaitis, P. J. (2017). Downscaling soil moisture over regions that include multiple coarse-resolution grid cells. Remote Sensing of Environment, 199, 187-200. https://doi.org/10.1016/j.rse.2017.07.021

Jin, Y., Ge, Y., Liu, Y., Chen, Y., Zhang, H., & Heuvelink, G. B. (2020). A machine learning-based geostatistical downscaling method for coarse-resolution soil moisture products. IEEE Journal of Selected Topics in Applied Earth Observations and Remote Sensing, 14, 1025-1037. https://doi.org/10.1109/JSTARS.2020.3035386

Johnson, M. G., & Beschta, R. L. (1980). Logging, infiltration capacity, and surface erodibility in western Oregon. Journal of Forestry, 78(6), 334-337. https://doi.org/10.1093/jof/78.6.334

Mascaro, G., Vivoni, E. R., & Deidda, R. (2010). Downscaling soil moisture in the southern Great Plains through a calibrated multifractal model for land surface modeling applications. Water Resources Research, 46(8). https://doi.org/10.1029/2009WR008855

Merlin, O., Chehbouni, A., Kerr, Y. H., & Goodrich, D. C. (2006). A downscaling method for distributing surface soil moisture within a microwave pixel: Application to the

Monsoon'90 data. *Remote Sensing of Environment*, *101*(3), 379-389. https://doi.org/10.1016/j.rse.2006.01.004

Najafi, A., Solgi, A., & Sadeghi, S. H. (2010). Effects of skid trail slope and ground skidding on soil disturbance. Caspian Journal of Environmental Sciences, 8(1), 13-23. https://cjes.guilan.ac.ir/?_action=articleInfo&article=1030 `

Nash, J. E., & Sutcliffe, J. V. (1970). River flow forecasting through conceptual models part I—A discussion of principles. *Journal of hydrology*, *10*(3), 282-290. https://doi.org/10.1016/0022-1694(70)90255-6

O'Neill, P. E., S. Chan, E. G. Njoku, T. Jackson, R. Bindlish, J. Chaubell, and A. Colliander. (2021). SMAP Enhanced L3 Radiometer Global and Polar Grid Daily 9 km EASE-Grid Soil Moisture, Version 5 [Dataset]. Boulder, Colorado USA. NASA National Snow and Ice Data Center Distributed Active Archive Center. https://doi.org/10.5067/4DQ54OUIJ9DL.

Pauly, M. J., 2019. Modeling and field evaluation of the strength of surface soils for vehicle mobility. Master's Thesis, Colorado State University, Fort Collins, CO.

Pauly, M. J., Niemann, J. D., Scalia, J., Green, T. R., Erskine, R. H., Jones, A. S., & Grazaitis, P. J. (2020). Enhanced hydrologic simulation may not improve downscaled soil moisture patterns without improved soil characterization. *Soil Science Society of America Journal*, *84*(3), 672-689. https://doi.org/10.1002/saj2.20052

Peng, J., Albergel, C., Balenzano, A., Brocca, L., Cartus, O., Cosh, M. H., ... & Loew, A. (2021). A roadmap for high-resolution satellite soil moisture applications–confronting product characteristics with user requirements. Remote Sensing of Environment, 252, 112162. https://doi.org/10.1016/j.rse.2020.112162

Perry, M. A., & Niemann, J. D. (2007). Analysis and estimation of soil moisture at the catchment scale using EOFs. Journal of Hydrology, 334(3-4), 388-404. https://doi.org/10.1016/j.jhydrol.2006.10.014

Ranney, K. J., Niemann, J. D., Lehman, B. M., Green, T. R., & Jones, A. S. (2015). A method to downscale soil moisture to fine resolutions using topographic, vegetation, and soil data. Advances in Water Resources, 76, 81-96. https://doi.org/10.1016/j.advwatres.2014.12.003

Rezanezhad, F., Price, J. S., Quinton, W. L., Lennartz, B., Milojevic, T., & Van Cappellen, P. (2016). Structure of peat soils and implications for water storage, flow and solute transport: A review update for geochemists. *Chemical Geology*, *429*, 75-84. https://doi.org/10.1016/j.chemgeo.2016.03.010

Sabaghy, S., Walker, J. P., Renzullo, L. J., & Jackson, T. J. (2018). Spatially enhanced passive microwave derived soil moisture: Capabilities and opportunities. Remote Sensing of Environment, 209, 551-580. https://doi.org/10.1016/j.rse.2018.02.065

Sadeghi, S., Solgi, A., & Tsioras, P. A. (2022). Effects of traffic intensity and travel speed on forest soil disturbance at different soil moisture conditions. International Journal of Forest Engineering, 33(2), 146-154. https://doi.org/10.1080/14942119.2022.2055442

Schönauer, M., Ågren, A. M., Katzensteiner, K., Hartsch, F., Arp, P., Drollinger, S., & Jaeger, D. (2023). Predicting rut depth with soil moisture estimates from ERA5-Land and in-situ measurements. Zenodo. https://doi.org/10.5281/zenodo.8269412

Soil Survey Staff, Natural Resources Conservation Service, United States Department of Agriculture. Web Soil Survey. https://websoilsurvey.nrcs.usda.gov/. (Accessed April 2022)

USDA/NRCS, 2023. National Geospatial Center of Excellence. (n.d.). National Elevation Data 10 meter or better [Dataset]. Accessed 02-01-2023.

Werbylo, K. L., & Niemann, J. D. (2014). Evaluation of sampling techniques to characterize topographically-dependent variability for soil moisture downscaling. Journal of Hydrology, 516, 304-316. https://doi.org/10.1016/j.jhydrol.2014.01.030

Wu, X., Walker, J. P., Das, N. N., Panciera, R., & Rüdiger, C. (2014). Evaluation of the SMAP brightness temperature downscaling algorithm using active–passive microwave observations. Remote sensing of environment, 155, 210-221. https://doi.org/10.1016/j.rse.2014.08.021

Xu, W., Zhang, Z., Long, Z., & Qin, Q. (2021). Downscaling SMAP soil moisture products with convolutional neural network. IEEE Journal of Selected Topics in Applied Earth Observations and Remote Sensing, 14, 4051-4062. https://doi.org/10.1109/JSTARS.2021.3069774